processes

MDPI

Article

Hydrocarbon Generation and Residue Features of Ediacaran High-Maturity Source Rocks and Their Significance in Gas Exploration in Sichuan Basin

Wenyang Wang [1,*], Xiongqi Pang [2,3], Yaping Wang [3,4], Mingjun Chen [5], Ying Chen [1], Changrong Li [6] and Zhangxin Chen [7,*]

[1] State Key Laboratory of Lithospheric Evolution, Institute of Geology and Geophysics, Chinese Academy of Sciences, Beijing 100029, China
[2] State Key Laboratory of Petroleum Resources and Prospecting, China University of Petroleum (Beijing), Beijing 102249, China
[3] College of Geosciences, China University of Petroleum (Beijing), Beijing 102249, China
[4] Research Institute of Exploration and Development, PetroChina Southwest Oil & Gas Field Company, Chengdu 610041, China
[5] Petroleum Engineering School, Southwest Petroleum University, Chengdu 610500, China
[6] School of Earth and Space Sciences, Peking University, Beijing 100871, China
[7] Chemical and Petroleum Engineering, Schulich School of Engineering, University of Calgary, Calgary, AB T2N 1N4, Canada
* Correspondence: wywang@mail.iggcas.ac.cn (W.W.); zhachen@ucalgary.ca (Z.C.)

Abstract: Evaluating residual hydrocarbons is crucial for assessing shale oil and gas reservoirs, significantly impacting resource evaluation and exploration prospects. Previously regarded as lacking hydrocarbon generation potential, the Ediacaran Dengying Formation (Fm) microbial dolomite in the Sichuan Basin has been re-evaluated for its hydrocarbon generation capabilities. While understanding source rock characteristics is vital for petroleum resource assessment, a comprehensive analysis of the dolomite's source rocks, encompassing hydrocarbon generation and residual features, remains undocumented. In this study, we thoroughly analyze the total organic carbon and vitrinite reflectance and extensively utilize pyrolysis analysis, gas chromatography and isotopic analysis of the organic kerogen from the Ediacaran Dengying Fm dolomite samples. The findings affirm that the Ediacaran Dengying Fm dolomite indeed serves as a source rock with moderate hydrocarbon generation and residue capabilities. This microbial dolomite was formed in a reducing marine environment with high salinity. Characterized by an averaging TOC of 0.82%, the kerogen is primarily identified as type I, with a minor presence of type II, and underwent thermal maturation up to the post-maturity stage. Throughout its geological history, the maximum intensities for hydrocarbon generation and residues were 4.5×10^7 t/km^2 and 3.2×10^7 t/km^2, respectively. Additionally, cumulatively generated and residual hydrocarbon quantities amounted to 2.7×10^{12} t and 1.67×10^{12} t, respectively. This study indicates significant exploration potential for the Ediacaran Dengying Fm microbial dolomite. Consequently, the central region in the Sichuan Basin has been identified as a promising area for future exploration endeavors. Our study provides valuable insights for the understanding of shale gas exploration in high-maturity source rock areas.

Keywords: sichuan basin; precambrian petroleum system; high-maturity source rock; hydrocarbon residues; shale gas

check for updates

Citation: Wang, W.; Pang, X.; Wang, Y.; Chen, M.; Chen, Y.; Li, C.; Chen, Z. Hydrocarbon Generation and Residue Features of Ediacaran High-Maturity Source Rocks and Their Significance in Gas Exploration in Sichuan Basin. *Processes* **2023**, *11*, 3193. https://doi.org/10.3390/pr11113193

Academic Editor: Carlos Sierra Fernández

Received: 12 October 2023
Revised: 29 October 2023
Accepted: 3 November 2023
Published: 8 November 2023

1. Introduction

Interest in studying the petroleum systems of the Precambrian has grown significantly over the past decade [1–6]. These areas garnered attention as prospective exploration sites after the discovery of a multitude of vast oil and gas fields in China, Africa, eastern Europe, Russia, Arabia, and Oman [7–12]. Significant natural gas accumulation has been recently discovered within the dolomite units in the Ediacaran Dengying Fm in the Sichuan Basin, which represents a new and important supplement to the worldwide ancient Precambrian petroleum systems. These systems are known for their extensive reserves and production, at 4.0×10^{11} m^3 [4,12–14].

Significant quantities of shale gas are found within high-maturity source rocks [15]. The potential of shale oil and gas resources within these rocks is determined via residual hydrocarbons [16]. The assessment of residual hydrocarbons plays a crucial role in evaluating shale oil and gas resources and selecting exploration prospects [17–19]. Previous studies suggest that the Ediacaran Dengying Fm acted as a reservoir in the Sichuan Basin. The overlying Cambrian formation contains the source rock of mud shale [20–22], from which the Ediacaran gas was derived. However, extensive research and drilling activities conducted in the Ediacaran Dengying Fm microbial dolomite in recent years have provided novel insights. First, the proven gas reserves that currently occur in Ediacaran rock [4,12,14] are more than twice the size of the predicted gas resources (1.7×10^{11} m^3) of the third resource assessment conducted by PetroChina Southwest Oil and Gas Fields. This indicates a contribution from other sources in addition to the Cambrian Qiongzhusi Formation source rock of mud shale. Second, studies on trace elements, carbon and oxygen isotopes, and pyrite have proved that the paleo–sedimentary environment and preservation conditions were sufficiently favorable to enable the Dengying microbial dolomite to form a good source rock [23,24]. The co-existence of native bitumen in this dolomite facies proves that hydrocarbon generation occurred during its geologic history [22,25,26]. Third, the natural gas geochemistry and source correlation indicate that the microbial dolomite provides the most important source contribution to the Dengying gas accumulation [1].

There is growing research pointing to the potential of dolomite as a source rock for hydrocarbons around the world. Peters et al. (1995) highlighted the possibility of substantial petroleum generation from the marine algal-laminated dolomites of the Infracambrian Bilara Formation in the Bikaner-Nagaur basin in India [27]. These dolomites were found to be marginally mature (with Tmax values of 436 °C or less), containing moderate to high total organic carbon (TOC) levels, and exhibiting hydrogen indices typical of oil-prone organic material, reaching up to 400 mg hydrocarbon per gram of TOC. Słowakiewicz and Mikołajewski (2011) discussed the potential of dolomite microbialites as a source of hydrocarbons within the Zechstein (Upper Permian) Main Dolomite carbonates in the western part of the Polish sector of the Southern Permian Basin [28]. Calculations suggested original TOC values ranging from 0.8 to 2.0 weight percent, with type II kerogen present and varying thermal maturities between 0.85% and 3.2% R_o. Pan et al. (2020) presented findings on the hydrocarbon generation potential of dolomite within the Permian Lucaogou Formation in the Malang Sag, Santanghu Basin, Western China [29]. These dolomites exhibited total organic carbon (TOC) values ranging from 0.8 to 7.3% (averaging 2.7%), they contained Type I and II1 kerogen, were in the early mature to mature stage of thermal maturity, and had hydrogen index (HI) values spanning from 142 to 975 mg/g.

These discoveries have prompted more scientists to redefine the Ediacaran Dengying microbial dolomite as a set of potential source rocks in the Sichuan Basin [1,4,12,13,30,31]. A thorough assessment of these source rocks, focusing on hydrocarbon generation and residual potential, captured the attention of oil explorers. In the investigation conducted by Zou et al. [1], an analysis of microbial dolomite source rock quality was conducted utilizing data from outcrops, core samples, drilling cuttings, and seismic data. In the research of Shi et al. [4], they preliminarily addressed the hydrocarbon generation capability of Ediacaran source rocks according to TOC, pyrobitumen reflectance, and kerogen carbon isotope analyses. However, the quantitative analysis of the hydrocarbon generation and residue features of the Ediacaran Dengying Fm source rocks during the geologic history is absent from the literature.

Evaluation of the hydrocarbon generation and residue quantities in source rocks has previously been experimentally conducted [32–35]. However, the simulation results of hydrocarbon generation differ significantly because the parameters differ according to the kerogen types [36–38]. Therefore, the simulation of the hydrocarbon generation of a sample cannot accurately reflect the hydrocarbon generation capacity of the source rock that is distributed across the entire basin [38]. In addition, accurately measuring the hydrocarbon generation quantities and residue quantities in source rocks throughout geological history for experimental simulations becomes complex when multiple phases of hydrocarbon generation have occurred [39].

This study intends to quantify the hydrocarbon generation and residue features of the Ediacaran Dengying Fm dolomite in the Sichuan Basin. The goals of this study encompass (1) systemically evaluation of the geological features of this facies including the sedimentary environment, areal distribution, as well as the characteristics of organic matter abundance, organic matter type, and organic matter thermal maturity; (2) quantitative analysis of the hydrocarbon generation and residue features of this dolomite that occurred during its geologic history and (3) computation of the quantities of hydrocarbon generation and residues of the Ediacaran Dengying Fm dolomite, and forecasts of promising zones for targeted exploration strategies.

2. Geological Setting

The Sichuan Basin, located in the Sichuan province of Western China, encompassing an area of approximately 1.9×10^5 km^2, is a prominent gas-rich petroliferous basin formed atop the Upper Yangtze Craton [40]. Situated in a tectonically intricate region, the northwest border of the basin is adjacent to the Longmenshan fault zone, while the northeast border of the basin abuts the Dabashan fault zone. The basin's location at the convergence of multiple plates contributes to its complex tectonic dynamics. The Sichuan Basin, with respect to tectonic movement, is partitioned into six distinct structural units, namely the western, northern, central, southwestern, southern, and eastern districts (Figure 1) [12,41,42]. Over different geological periods, the Sichuan Basin has undergone five major tectonic movements corresponding to significant evolutionary stages [4]. The regional tectonic stress has experienced two distinct stages: the initial stage from Ediacaran to Early Triassic, characterized by a tensile stress environment, and the subsequent stage from Middle Triassic to Quaternary, dominated by compressive stress [43].

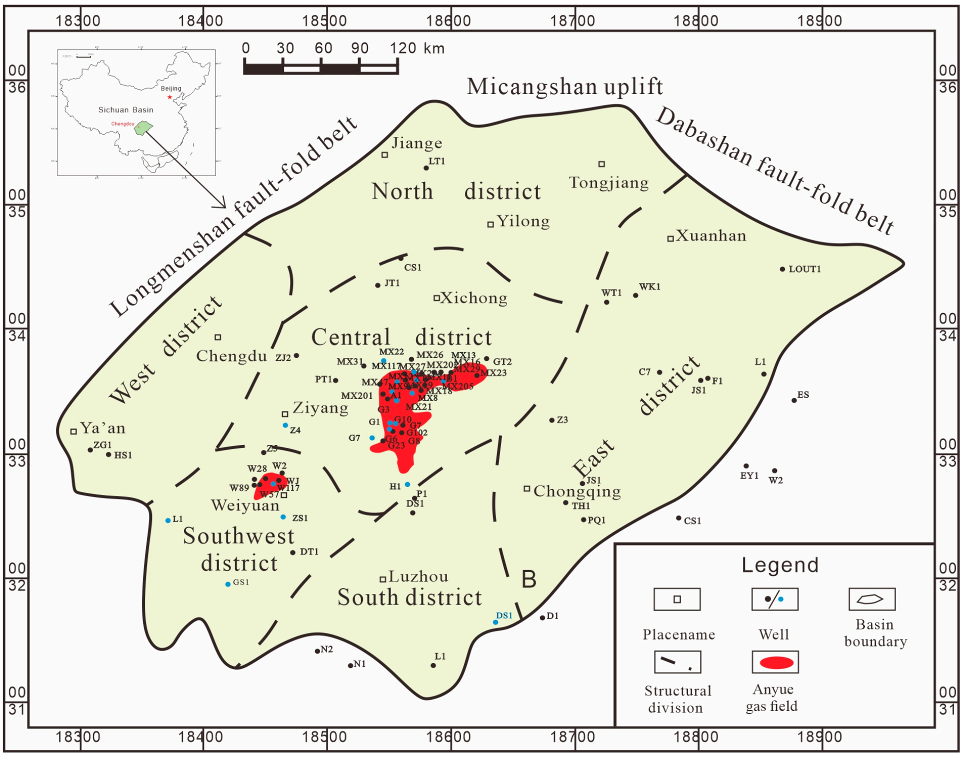

Figure 1. Location and structural map of the Sichuan Basin (Revised from Ref. [12]). The blue wells are the sampling wells in this study.

The Ediacaran strata found in the Sichuan Basin consist of the Upper Dengying Formation and the Lower Doushantuo Formation [12,44]. This study primarily focuses on the Dengying Formation, characterized by a sedimentary environment, mostly comprising a carbonate platform. The dominant lithology is dolomite, categorized as Zd^1 to Zd^4 from bottom to top (Figure 2). Zd^1 primarily consists of microbial dolomite with a minor presence of crystal powder dolomite. Zd^2 is predominantly microbial dolomite, followed by powder dolomite, and contains a small amount of dolomite mudstone. Zd^3 is composed of shale with thin siliceous dolomite, while Zd^4 is dominated by powder crystal dolomite, with microbial dolomite also present [1,4]. The Ediacaran System in the Sichuan Basin holds substantial natural gas resources and presents promising exploration prospects. According to Du et al. [45], the estimated gas reserves of the Ediacaran Dengying Formation range from 0.66 to 1.37 × 10^{12} m^3.

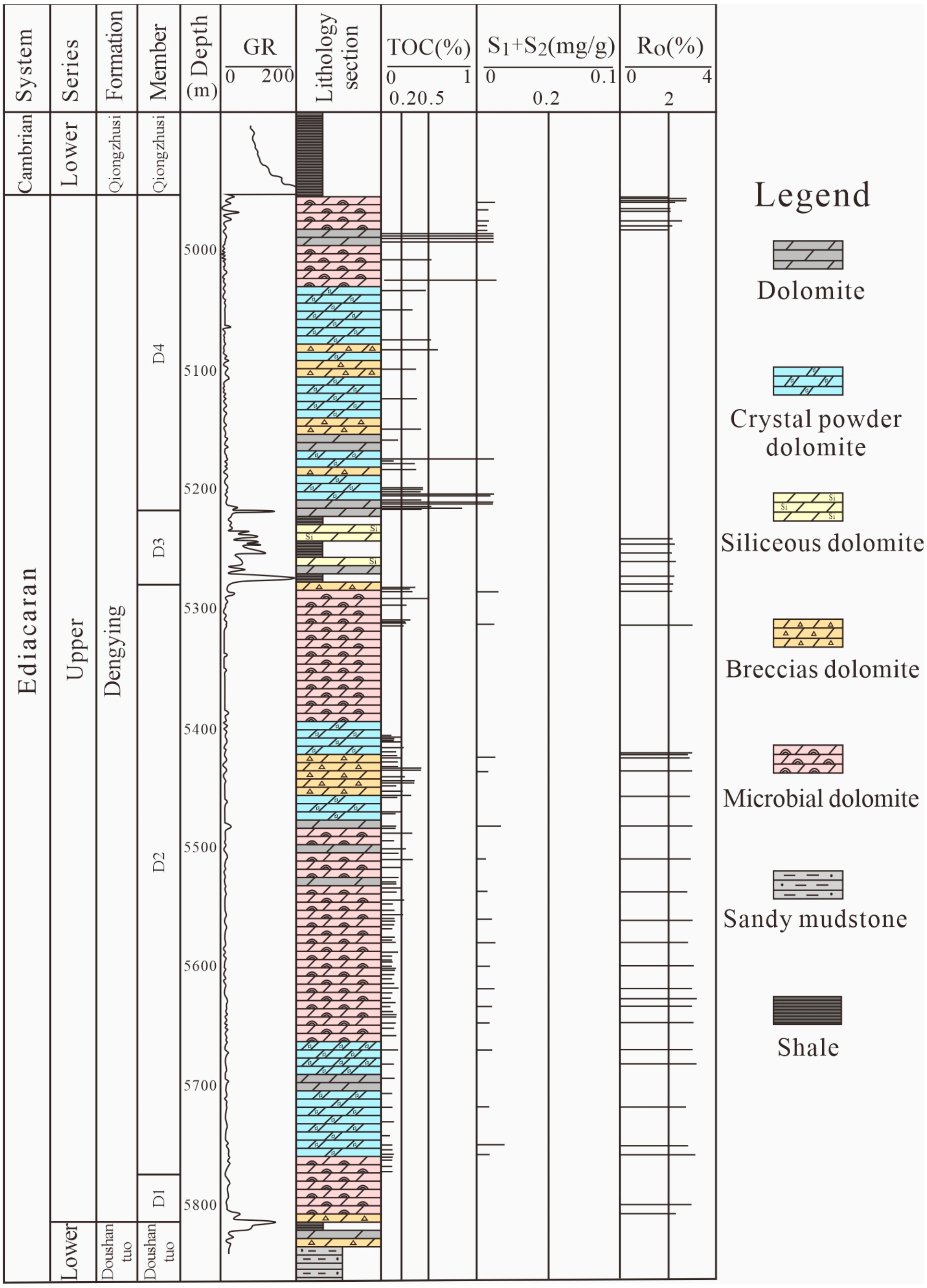

Figure 2. Precambrian geochemical profile of well W117 in the central area of the Sichuan basin. The location of well W117 is shown in Figure 1.

3. Data and Methods

3.1. Data

Various geological and geochemical data were amassed in this study. On the geological front, the information includes the burial and thermal evolution history, the density, residual thickness and range of distribution of the Ediacaran Dengying Formation microbial dolomite of the Sichuan basin. For geochemical data, these encompass experimental data such as the total organic carbon (TOC) and vitrinite reflectance, and the results of pyrolysis analysis, gas chromatography, and isotopic analysis of organic kerogen. Some of the data utilized in this study originate from previous studies [4,46,47].

3.2. Sample Preparation and Experiments

The samples were collected from the PetroChina Southwest Oil and Gas Field Company. The process for preparing samples for TOC analyses adhered to established procedures as outlined in Stüeken et al. (2017) [48]. Approximately 0.2 g of powdered rock was carefully measured and placed into glass centrifuge tubes, which had been pre-treated in a muffle furnace at 900 °C for 2 h. Subsequently, 10 mL of 6N HCl was added to the tubes, and the mixture was stirred using a glass rod, followed by a 10-min sonication. The samples were allowed to react overnight at a temperature of 60 °C. To ensure complete dissolution of the soluble carbonate phases, the HCl solution was replaced three times. After this, the samples were centrifuged, the acidic solution was poured off, and the powdered residue was washed four times with deionized water (DI-H_2O) to eliminate any remaining chloride. The decarbonated samples were then dried via baking at 60 °C for 4 h [49].

Prior to the isolation of kerogen, the powdered samples underwent a chloroform extraction in a Soxhlet extractor at 80 °C for 48 h to extract soluble organic materials. The isolation of kerogen followed the methodologies described by Durand (1980) and Vandenbroucke and Largeau (2007) [50,51]. Approximately 10 g of the previously extracted sample powder was subjected to a treatment with 6 N HCl to eliminate carbonate, sulfide, sulfate, and hydroxides. Subsequently, the samples were treated with a mixture of 40% HF and 6 N HCl to dissolve clay minerals and silicates, followed by a second treatment with 6 N HCl. Following these treatments, the samples were rinsed until they reached a neutral state and then dried at a temperature of 100 °C [49]. Once the samples were completely dry, the concentrate was homogenized through grinding in preparation for the isotopic analysis of organic kerogen.

The TOC of all samples was evaluated using a carbon/sulfur analyzer (Series CS230; LECO, St. Joseph, MO, USA), and the organic matter was burned and converted to CO_2 at 900 °C [47,52]. Using Rock-Eval pyrolysis, the samples were placed in a crucible, with N_2 as the carrier gas; using a specific heating program, the rock was heated at 300 °C for 3 min, and the free hydrocarbon content (S_1) was obtained. In the temperature range of 300–600 °C, the pyrolysis hydrocarbon content (S_2) was obtained by heating at 25 °C/min, the data was from Ref. [47] (Table 1). The test instrument of the gas chromatography was the thermoelectric TRACE 1300 gas chromatograph. Test conditions: carrier gas 99.999% N_2 (flow rate 1 mL/min), combustion gas H_2, injection port and FID detector temperature of 300 °C. The R_o was measured using an MPV-SP microphotometer (Table 2), the data was from Ref. [47]. The isotopic analysis of organic kerogen was conducted using a Thermo Scientific FLASH 2000 elemental analyzer coupled to a MAT 253 continuous-flow isotope-ratio mass spectrometer (IRMS) via a Conflo IV interface.

Table 1. TOC and Rock-Eval pyrolysis data of the Ediacaran microbial dolomite.

Sample	Depth (m)	S_1 (mg/g)	S_2 (mg/g)	$S_1 + S_2$ (mg/g)	TOC (%)	HI (mg HC/g TOC)
#1	5030	0.57	0.13	0.7	3.04	4
#2	5042	0.49	0.11	0.6	3.42	3
#3	5295	0.76	0.9	1.66	1.68	54
#4	5029	0.71	0.71	1.42	5.23	14
#5	5070	1.28	0.69	1.97	3.11	22
#6	5163	0.1	0.08	0.18	3.03	3
#7	5095	0.75	0.7	1.45	3.84	18
#8	5175	1.65	1.23	2.88	1.6	77
#9	5215	1.35	0.69	2.04	1.54	45
#10	5352	0.22	0.2	0.42	1.01	20
#11	5485	0.25	0.45	0.7	1.35	33
#12	5525	0.67	0.27	0.94	1.48	18
#13	5394	0.04	0.04	0.08	1.08	4
#14	3169	0.16	0.12	0.28	1.27	9
#15	3193	0.12	0.17	0.29	1.04	16

Table 1. *Cont.*

Sample	Depth (m)	S_1 (mg/g)	S_2 (mg/g)	$S_1 + S_2$ (mg/g)	TOC (%)	HI (mg HC/g TOC)
#16	3218	0.15	0.19	0.34	1.06	18
#17	4427	0.67	1.88	2.55	1.12	168
#18	4439	1.42	1.36	2.78	1.41	96
#19	4458	0.24	0.2	0.44	1.81	11
#20	4470	1.1	0.79	1.89	1.92	41
#21	4481	0.88	2.01	2.89	1.78	113
#22	4490	1.2	2.24	3.44	0.75	299
#23	4509	0.98	0.9	1.88	1.66	54
#24	4626	0.61	0.35	0.96	0.58	60
#25	4679	0.62	0.27	0.89	0.22	123
#26	4710	0.21	0.15	0.36	0.55	27
#27	4735	0.14	0.11	0.25	0.57	19
#28	4770	0.12	0.09	0.21	0.53	17
#29	4805	0.14	0.18	0.32	0.55	33
#30	4840	0.26	0.3	0.56	0.49	61
#31	4875	0.87	0.36	1.23	0.41	88
#32	4901	0.07	0.05	0.12	0.38	13
#33	4921	0.08	0.07	0.15	0.35	20
#34	5137	0.7	0.72	1.42	2.54	28
#35	5237	0.37	0.61	0.98	3.35	18
#36	5287	0.35	0.25	0.6	2.22	11
#37	5337	0.35	0.28	0.63	1.8	16
#38	5387	0.67	0.46	1.13	5.49	8
#39	5537	0.12	0.07	0.19	1.04	7
#40	5150	0.8	1.09	1.89	2.09	52
#41	5200	0.38	0.45	0.83	1.81	25
#42	5250	0.34	0.54	0.88	2.74	20
#43	5350	0.24	0.09	0.33	0.93	10
#44	5400	0.47	0.62	1.09	0.8	78
#45	5450	0.44	0.25	0.69	1.02	25
#46	5101	0.55	0.4	0.95	2.36	17
#47	5301	1	0.87	1.87	1.64	53
#48	5085	0.21	0.29	0.5	1.52	19
#49	5001	1.48	0.79	2.27	3.02	26
#50	5035	1.73	1.69	3.42	2.26	75
#51	5141	0.37	0.31	0.68	1.36	23
#52	5241	0.4	0.38	0.78	1.76	22
#53	5341	0.32	0.24	0.56	0.84	29
#54	5129	0.5	0.39	0.89	1.79	22
#55	5229	0.17	0.43	0.6	1.85	23
#56	5329	0.54	0.24	0.78	1.06	23
#57	5429	0.18	0.37	0.55	0.96	39
#58	5451	0.39	0.31	0.7	1.18	26
#59	5631	0.28	0.29	0.57	1.04	28
#60	5681	0.33	0.33	0.66	1.14	29
#61	5112	1	1.32	2.32	2.54	52
#62	5132	0.99	1.57	2.56	2.67	59
#63	5162	0.75	0.64	1.39	2.63	24
#64	5192	0.26	0.41	0.67	2.23	18
#65	5222	0.51	1.03	1.54	2.85	36
#66	5426	0.04	0.04	0.08	1.88	2
#67	5442	0.16	0.24	0.4	1.83	13
#68	5502	0.1	0.1	0.2	2.07	5
#69	5532	0.21	0.44	0.65	2.27	19
#70	5562	0.06	0.1	0.16	1.72	6
#71	5592	0.31	0.17	0.48	1.55	11

Table 1. *Cont.*

Sample	Depth (m)	S_1 (mg/g)	S_2 (mg/g)	$S_1 + S_2$ (mg/g)	TOC (%)	HI (mg HC/g TOC)
#72	5622	0.36	0.77	1.13	1.77	44
#73	5652	0.16	0.27	0.43	1.45	19
#74	5682	0.16	0.29	0.45	1.3	22
#75	5732	0.44	0.39	0.83	1.68	23
#76	5762	0.67	0.6	1.27	2.01	30
#77	5792	0.5	0.5	1	1.61	31
#78	5852	0.33	0.25	0.58	1.79	14
#79	5912	0.32	0.59	0.91	2.02	29
#80	5022	3.91	1.05	4.96	6.33	17
#81	5045	0.22	0.19	0.41	3.23	6
#82	5082	0.22	0.37	0.59	1.49	25
#83	5435	0.03	0.03	0.06	1.51	2
#84	5462	0.23	0.95	1.18	1.33	71
#85	3014	0.19	0.22	0.41	1.44	15
#86	2989	0.05	0.09	0.14	0.24	38
#87	3010	0.03	0.04	0.07	0.26	15
#88	3013	0.04	0.03	0.07	0.17	18
#89	3015	0.05	0.03	0.08	0.68	4
#90	3034	0.05	0.03	0.08	0.32	9
#91	3073	0.02	0.04	0.06	0.15	27
#92	3080	0.11	0.2	0.31	0.25	80
#93	3114	0.03	0.02	0.05	0.14	14
#94	3267	0.03	0.03	0.06	0.12	25
#95	3346	0.02	0.02	0.04	0.11	18
#96	3354	0.03	0.02	0.05	0.39	5
#97	3370	0.03	0.03	0.06	0.14	21
#98	3430	0.02	0.02	0.04	0.1	20
#99	3502	0.06	0.05	0.11	0.33	15
#100	3531	0.13	0.21	0.34	0.13	162
#101	3547	0.07	0.06	0.13	0.08	75
#102	3605	0.58	0.92	1.5	1.45	63
#103	3639	0.01	0.03	0.04	0.11	27
#104	3687	0.04	0.02	0.06	0.26	8
#105	3740	0.06	0.15	0.21	0.05	300
#106	3792	0.02	0.01	0.03	0.07	14
#107	3821	0.03	0.02	0.05	0.07	29
#108	3877	0.03	0.01	0.04	0.05	20
#109	3915	0.03	0.04	0.07	0.04	100
#110	3964	0.11	0.47	0.58	0.09	522
#111	3978	1.34	0.76	2.1	0.69	110
#112	4019	0.08	0.11	0.19	0.13	85
#113	4075	0.04	0.07	0.11	0.21	33
#114	3047	0.37	0.32	0.69	1.53	21
#115	5314	0.02	0.04	0.06	1.96	2
#116	5354	0.23	0.27	0.5	2.66	10
#117	5112	0.08	0.04	0.12	1.96	2
#118	5112	0.03	0.02	0.05	0.05	40
#119	5202	0.06	0.16	0.22	0.22	73

Table 2. Vitrinite reflectance data of Ediacaran source rocks in Sichuan basin [47].

Well	Depth (m)	R_{min} (%)	R_{max} (%)	R_o %	Counts	Well	Depth (m)	R_b (%)	R_{eq} (%)
Ap1	5030.17	2.63	2.68	2.65	20	Mx9	4964.77	3.29	2.43
Gs1	5295.00	2.53	2.61	2.59	20	Gk1	5356.73	3.45	2.53
Gs102	5029.00	2.57	2.63	2.61	20	Gs17	4969.42	3.53	2.58
Gs102	5070.49	2.55	2.59	2.57	20	Gs17	4985.10	3.60	2.63

Table 2. *Cont.*

Well	Depth (m)	R_{min} (%)	R_{max} (%)	R_o %	Counts	Well	Depth (m)	R_b (%)	R_{eq} (%)
Gs7	5351.85	2.57	2.60	2.60	20	-	-	-	-
Hs1	5394.10	2.55	2.62	2.59	20	-	-	-	-
Hs1	5753.58	2.56	2.60	2.58	20	-	-	-	-
Mx10	5387.00	2.55	2.65	2.60	20	-	-	-	-
Mx11	5150.00	2.58	2.63	2.61	20	-	-	-	-
Mx13	5341.00	2.65	2.75	2.70	10	-	-	-	-
Mx17	5129.00	2.53	2.61	2.57	10	-	-	-	-
Mx8	5425.68	2.70	2.85	2.78	20	-	-	-	-
Mx9	5045.07	2.73	2.91	2.82	20	-	-	-	-
Mx9	5435.20	2.59	2.64	2.61	20	-	-	-	-
Zs1	5314.24	2.73	2.90	2.86	20	-	-	-	-

The equivalent vitrinite reflectance (R_{eq}) transformed from pyrobitumen reflectance (R_b) was used in some samples; $R_{eq} = 0.618 \times R_b + 0.4$.

3.3. Conceptual Model

The hydrocarbon generation process in source rocks upholds the principle of mass conservation. The overall material quantity remains constant during the conversion of organic materials, which are transformed to be hydrocarbons within source rocks. The organic materials transformed to be hydrocarbons, i.e., hydrocarbon generation, consist of two parts: the hydrocarbons remaining within the source rock, referred to as residual hydrocarbons, and the hydrocarbons that have migrated out of the source rock, known as hydrocarbon expulsion. A traditional model is that suggested by Pang et al. [53], which quantitatively characterizes the generation and expulsion of hydrocarbons from source rocks, and has been widely applied in previous research [54,55]. However, this model is only applicable for assessing source rocks with low levels of maturity. Based on the traditional model, an improved model was established and used in the present study, as shown in Figure 3. In this new model, no pyrolysis data from low-maturity source rocks were required.

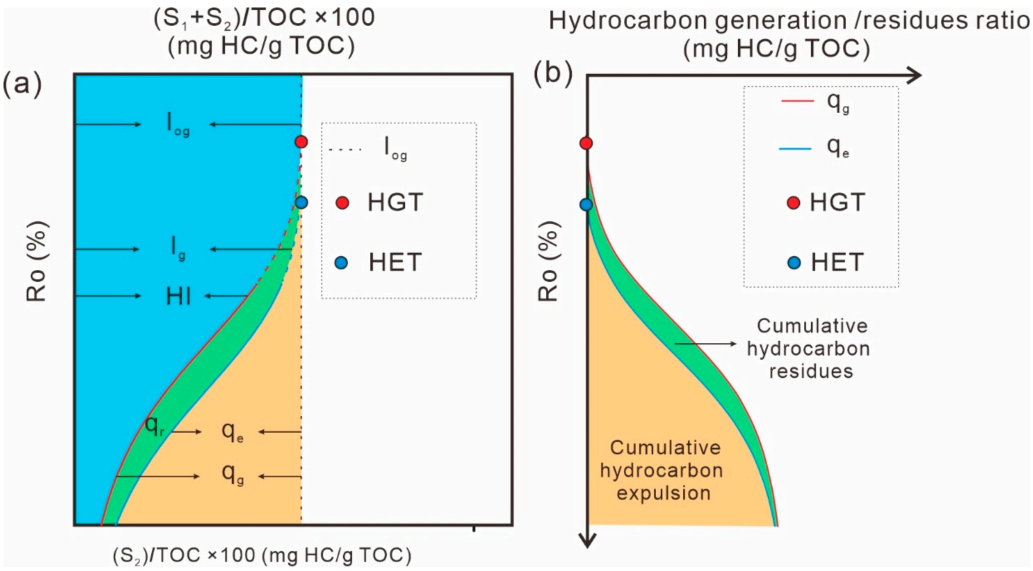

Figure 3. Conceptual model to compute the hydrocarbon generation and residue potential. HGT represents the threshold for hydrocarbon generation, while HET stands for the threshold for hydrocarbon expulsion. (**a**) The hydrocarbon generation potential index and the hydrogen index change with depth. (**b**) The hydrocarbon generation ratio and hydrocarbon residue ratio change with depth.

As source rocks mature, the organic matter within them gradually transforms into hydrocarbons. In this study, the hydrocarbon generation potential index (I_g, calculated as $(S_1 + S_2)/TOC$ [56]) reflects the potential for hydrocarbon generation per unit of organic carbon in source rocks. It encompasses both residual hydrocarbons and hydrocarbons that can further evolve with increasing maturity [53]. The hydrogen index (HI, calculated as S_2/TOC) represents the potential for additional hydrocarbon transformation per unit of organic carbon in source rocks. HGT refers to the maturity at which source rocks commence hydrocarbon generation. HET refers to the maturity at which point source rocks begin to expel hydrocarbons.

The hydrocarbon generation potential index corresponding to HET is denoted as I_{og}. I_{og} remains constant before reaching HET. After the release of hydrocarbons from source rocks, I_{og} begins to decrease. The difference between I_{og} and HI is defined as the hydrocarbon generation ratio (q_g), representing the hydrocarbons produced for each unit of organic carbon below the HGT (Equation (1)). Similarly, the disparity between I_{og} and I_g is referred to as the hydrocarbon expulsion ratio (q_e), signifying the hydrocarbons expelled for each unit of organic carbon below the HET (Equation (2)). Lastly, the difference between q_g and q_e yields the hydrocarbon residue ratio (q_r), illustrating the residual hydrocarbons for each unit of organic carbon below the HGT (Equation (3)).

$$q_g(R_o) = I_{og} - HI(R_o) \tag{1}$$

$$q_e(R_o) = I_{og} - I_g(R_o) \tag{2}$$

$$q_r(R_o) = q_g(R_o) - q_e(R_o) \tag{3}$$

In the above equations, q_g is the hydrocarbon generation ratio, measured in mg/g; q_e is the hydrocarbon expulsion ratio, measured in mg/g; q_r is the hydrocarbon residue ratio, measured in mg/g; I_{og} is the original hydrocarbon generation potential index, measured in mg/g; HI is the hydrogen index, measured in mg/g; I_g is the hydrocarbon generation potential index, measured in mg/g; R_o is the vitrinite reflectance, measured in %.

All calculation processes are completed in Doublefox Software. The input parameters consist of the values of q_g and q_r, total organic carbon (TOC), source rock thickness, source rock density, hydrocarbon generation ratio, and hydrocarbon residue ratio. As per Equations (4) and (5), the outputs are hydrocarbon generation intensity and residual hydrocarbon intensity, respectively. When the input parameters encompass the values of q_g and q_r, total organic carbon (TOC), source rock thickness, source rock density, source rock area data, hydrocarbon generation ratio, and hydrocarbon residue ratio, as described in Equations (6) and (7), the results are hydrocarbon generation amount and hydrocarbon residue amount.

$$H_g = \int_{{R_o}^t}^{R_o} 10^{-3} \times q_g(R_o) \times H \times \rho \times TOC_o(R_o) \times d(R_o) \tag{4}$$

$$H_r = \int_{{R_o}^t}^{R_o} 10^{-3} \times q_r(R_o) \times H \times \rho \times TOC_o(R_o) \times d(R_o) \tag{5}$$

$$Q_g = \int_{{R_o}^t}^{R_o} 10^{-13} \times q_g(R_o) \times H \times A \times \rho \times TOC_o(R_o) \times d(R_o) \tag{6}$$

$$Q_r = \int_{{R_o}^t}^{R_o} 10^{-3} \times q_r(R_o) \times H \times A \times \rho \times TOC_o(R_o) \times d(R_o) \tag{7}$$

In the above equations, H_g is the hydrocarbon generation intensity, measured in 10^4 t/km^2; H_r is the hydrocarbon residue intensity, measured in 10^4 t/km^2; H is the thickness of the source rock, measured in m; ρ is the density of the source rock, measured in g/cm^3; A is the area of source rocks, measured in km^2; TOC_o is the original TOC, measured in %; Q_g is the amount of hydrocarbon generation, measured in 10^8 t; Q_r is the amount of hydrocarbon residue, measured in 10^8 t.

To accurately reflect the original TOC [57], restoration is required, utilizing Equations (8) and (9).

$$TOC_o = TOC \times k \quad (8)$$

$$k = (1 - 0.83 \times \frac{I_g}{1000}) / \left(1 - 0.83 \times I_{og}/1000\right) \quad (9)$$

The study employed the Easy%R_o chemical kinetic model to establish the correlation between source rock thermal maturity and depth within the Sichuan Basin. This correlation was achieved through the utilization of basin simulation software, such as PetroMod and Basinmod. The burial and thermal histories of the source rock of the Ediacaran Dengying Formation were shown in Zou et al. [1]. The vitrinite reflectance data for the Ediacaran microbial dolomite source rock in the Sichuan Basin were determined using Equation (10) presented by Wang et al. [47] and was based on the findings discussed in Zou et al. [1].

$$R_o = 0.31 \times \exp\,(0.0004 \times Z) \quad (10)$$

In the above equation, R_o is the vitrinite reflectance, measured in %; Z is the depth of source rock, measured in m.

4. Results

4.1. Geological and Geochemical Features of Source Rocks

4.1.1. Sedimentary Environment

The Ediacaran system contains the first stable cap rocks in the Yangtze Craton developed on the South China rift basin under a tensional regional tectonic background [58]. Owing to the influence of the basement fault, a north–south rifting trough developed between Moxi Gaoshiti and Weiyuan Ziyang in the southwestern Sichuan Basin, which controlled the deposition of the Dengying Formation; the deposition in the rifting trough was relatively thin [13]. The Sichuan area was a carbonate platform with shallow water conditions abundant in algae during the deposition of the Dengying Fm, ultimately leading to the formation of microbial dolomite deposits [59].

Pristane (Pr)/n-C17 and phytane (Ph)/n-C18 ratios serve as comprehensive markers utilized for identifying sedimentary environments, organic matter origin, and thermal maturity [60–62]. Figure 4a displays the cross-plot for the dolomite within the Dengying Fm. The cross-plot for the dolomite of the Dengying Fm is shown in Figure 4a. All samples fell in the area of a reducing environment. The range of Ph/n-C_{18} was 0.08 to 0.97 with an average of 0.68, and that of Pr/n-C_{17} was 0.12 to 0.96 with an average of 0.53, which represents marine organic matter with a high thermal maturity [61,63]. The n-alkanes of the microbial dolomite showed similar unimodal distribution patterns in the n-C_{13} to n-C_{33} interval, and the main carbon peak was between n-C_{17} and n-C_{24} (Figure 4b). This suggests that the primary organic matter precursors for the microbial dolomite were predominantly aquatic organisms [64]. The Pr/Ph ratio is a widely adopted biomarker index, offering insights into the sedimentary environment [65,66]. Specifically, Pr/Ph ratios below 1.0 suggest reducing environments, while ratios exceeding 1.0 indicate oxidizing conditions [65]. Gammacerane develops in both saline and reducing environments [67]. The microbial dolomite within the Dengying Formation exhibited characteristics such as a low Pr value, high Ph value, and elevated gammacerane content, with a Pr/Ph ratio below 1, collectively indicating a marine environment with high salinity and reducing conditions, as shown in Figure 5. Additionally, the proportions of C27, C28, and C29 regular steranes serve as indicators of the depositional environment and organic matter origin. Specifically, C27 regular steranes are primarily derived from plankton, while C29 regular steranes are predominantly derived from terrestrial higher plants [68]. However, C_{27} and C_{29} before the late Paleozoic may be derived from red algae and green algae [69]. In our study, the C_{27}/C_{29} sterane ratio was approximately 0.8. This implies that the proportion of green algae in the organic matter source of the microbial dolomite was relatively high, which indicates a reducing environment (Figure 5).

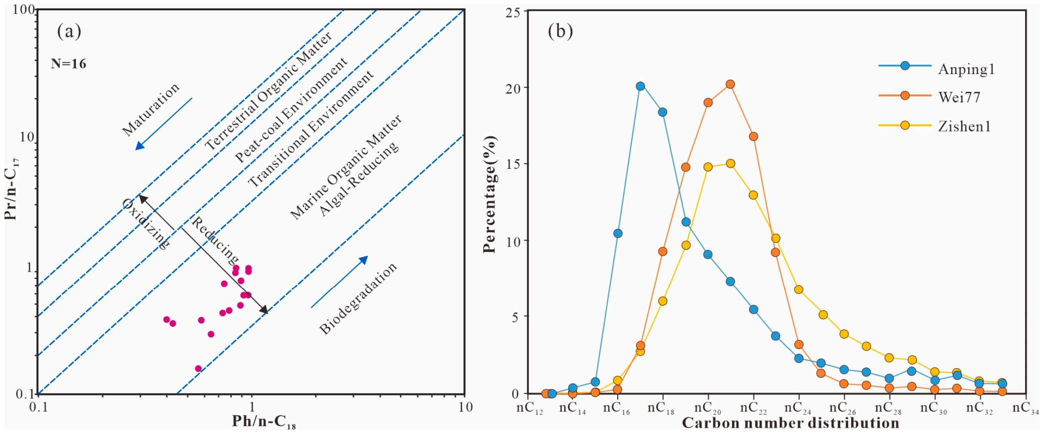

Figure 4. Sedimentary environment of microbial dolomite of the Dengying Formation. (**a**) Cross-plots of Ph/n-C18 versus Pr/n-C17 provide a visual representation to elucidate the sedimentary environment. (**b**) Carbon number distribution indicating the organic matter precursors.

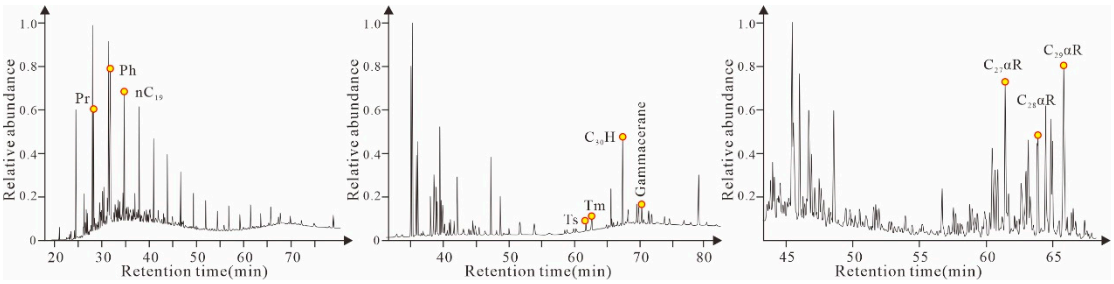

Figure 5. The outcomes of the gas chromatography–mass spectrometry experiment of the microbial dolomite in the Dengying Fm (Depth: 5047.2 m, Well Ap 2).

4.1.2. Geological Distribution

Beach facies rich in algae promote the development of dolomite abundant in algae, whereas sedimentary facies, such as semi-confined platforms, are unfavorable to its development. The central areas of the Sichuan basin are located in the dominant development area of microbial dolomite. This area is separated by semi-confined platforms with relatively undeveloped microbial dolomite [13], which control its thickness distribution. Figure 6 depicts the distribution of the microbial dolomite thickness within the Dengying strata. The thickness of the microbial dolomite of Dengying Fm spans from 80 m to 450 m, with an average of 251 m. Extensive development of microbial dolomite is observed in both the central regions and margins of the Sichuan Basin, reaching a maximum sedimentary thickness of 400 m. Because they are affected by differential denudation caused by tectonic activity, the sediments in the northeastern areas and northwestern areas of the Sichuan Basin are relatively thin, at only about 100 m in thickness.

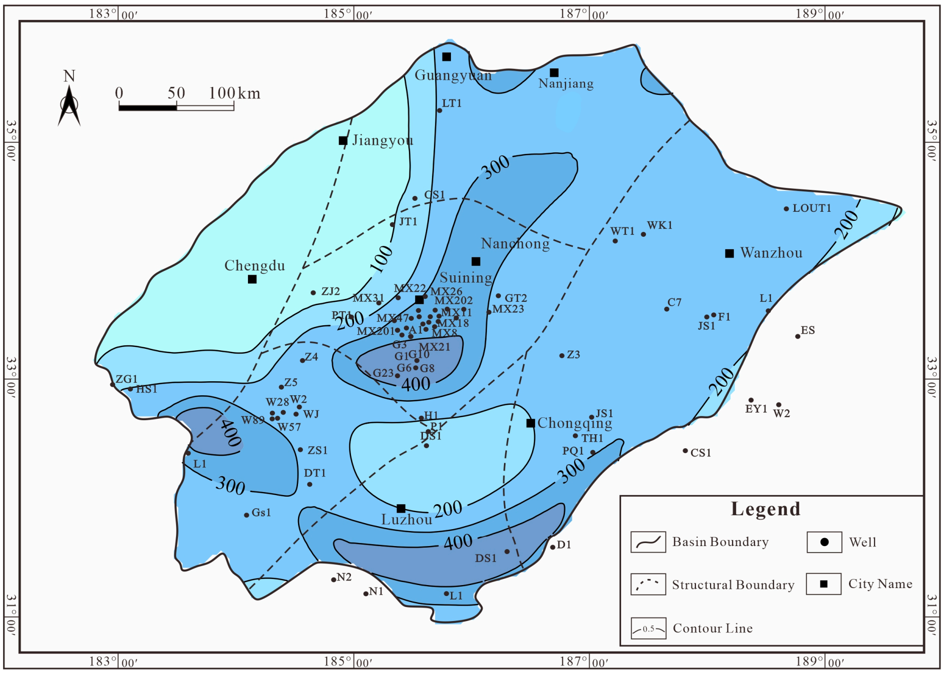

Figure 6. Thickness of the microbial dolomite of the Dengying Fm in the Sichuan Basin.

4.1.3. Organic Matter Abundance

Organic matter abundance is usually evaluated using the TOC [70]. The TOC of the Ediacaran Dengying Fm microbial dolomite varies greatly, with a maximum value of 4.0% and an average value of 0.82%. A total of 38.2% of the sample falls in the distribution interval from 0.5% to 1.0%, and 35.6% of the sample falls in the distribution interval of 0.2~0.5%. The distribution of TOC is also uneven in various regions within the basin. TOC in the central area of the basin is generally higher than in other areas, mainly in the range of 0.5% to 1% (Figure 7). According to the assessment criteria for highly mature marine carbonate source rocks established by Dai et al. [71], the Ediacaran Dengying Fm microbial dolomites are good source rocks; additionally, non-source rocks and poor source rocks are rare.

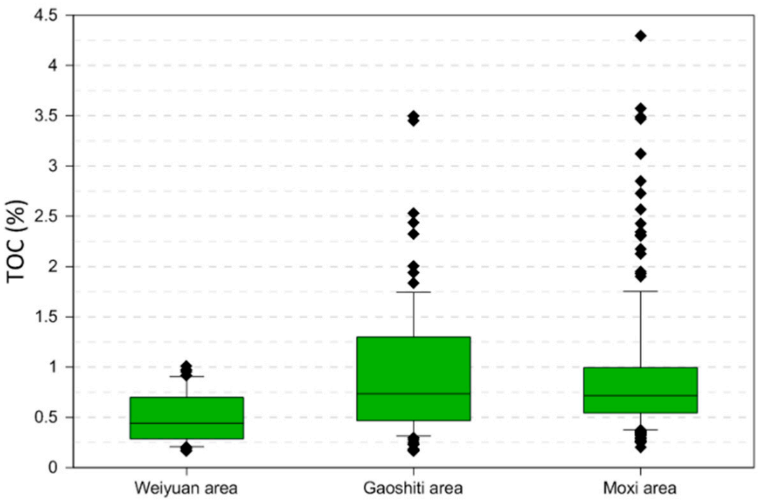

Figure 7. TOC of Ediacaran Dengying Fm microbial dolomite source rocks. The data were from Ref. [46].

4.1.4. Organic Matter Type

Kerogen types exhibit distinct compositions and structures, crucial in determining the potential for hydrocarbon generation. The composition and structure of kerogen vary based on kerogen types, directly influencing the potential for hydrocarbon generation and the type of hydrocarbons produced. Thermal evolution has a small effect on organic carbon isotopes and can also reflect the type of organic matter (SY/T 5735–1995) [72]. The carbon isotope of organic kerogen in the microbial dolomite was between −26.9‰ and −33.3‰ with an average value of 29.6‰, of which 85% was less than −28‰ (Figure 8). The results show that most of the microbial dolomites are type I kerogen (SY/T 5735–1995). This result is similar to the previous studies of Shi et al. [4] and Wang et al. [47]. They found that the microbial dolomite in the Dengying Fm predominantly consists of type I kerogen, characterized by high hydrocarbon generation potential. Furthermore, the analysis revealed that over 98% of the macerals in the microbial dolomite are sapropelic matter, reinforcing its classification as primarily type I kerogen, with type II being a rare occurrence.

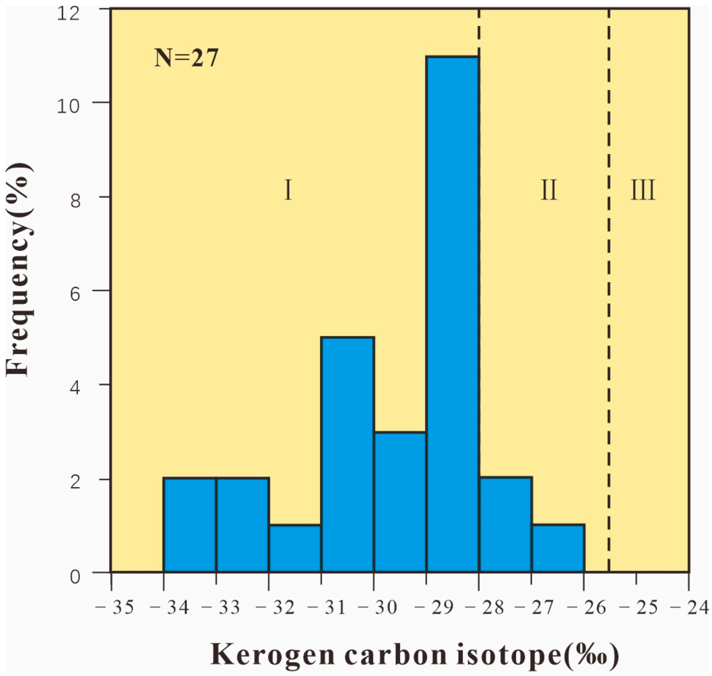

Figure 8. Kerogen carbon isotope histograms showing that the microbial dolomite is mainly Type I.

4.1.5. Organic Matter Thermal Maturity

The average vitrinite reflectance for the microbial dolomite within the Dengying Fm is 2.62%. This suggests that the microbial dolomite has progressed into the post-maturity stage. When considering regional variations, the thermal maturity in the central areas of the Sichuan Basin is notably higher, showcasing average R_o values of 2.66%. In contrast, the southwestern Sichuan Basin exhibits relatively lower thermal maturity, averaging 2.28% (Figure 9).

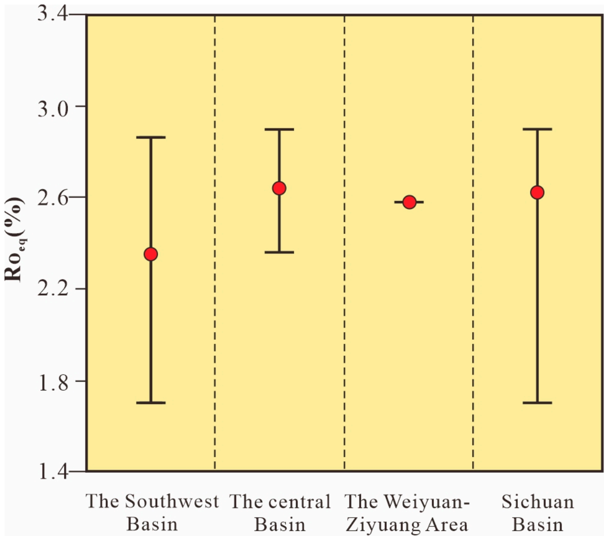

Figure 9. Thermal maturity of organic matter characteristics among areas. Circles depict the average data, while bars illustrate the data range. Some of the data utilized in this study originate in previous studies [4,46].

4.2. Hydrocarbon Generation and Residue Features of Source Rocks

4.2.1. Hydrocarbon Generation and Residue Model

Based on the Rock-Eval measurement data in conjunction with I_{og}, HGT, and HET, we established a model for hydrocarbon generation and residues in the Ediacaran Dengying Fm microbial dolomite source rocks. The observed pattern reveals that they enter the HGT stage at a R_o of 0.51%, initiating hydrocarbon generation and resulting in a decline in HI (Figure 10a). Subsequently, they enter the HET stage at a R_o of 0.92%, leading to a decrease in I_{og} (Figure 10a). Beyond a R_o of 3.5%, they cease to generate hydrocarbons, representing the lower limit of hydrocarbon generation (HLG). The I_{og} of Ediacaran Dengying Fm microbial dolomite source rocks was determined to be 756 mg HC/g TOC by Wang et al. [47].

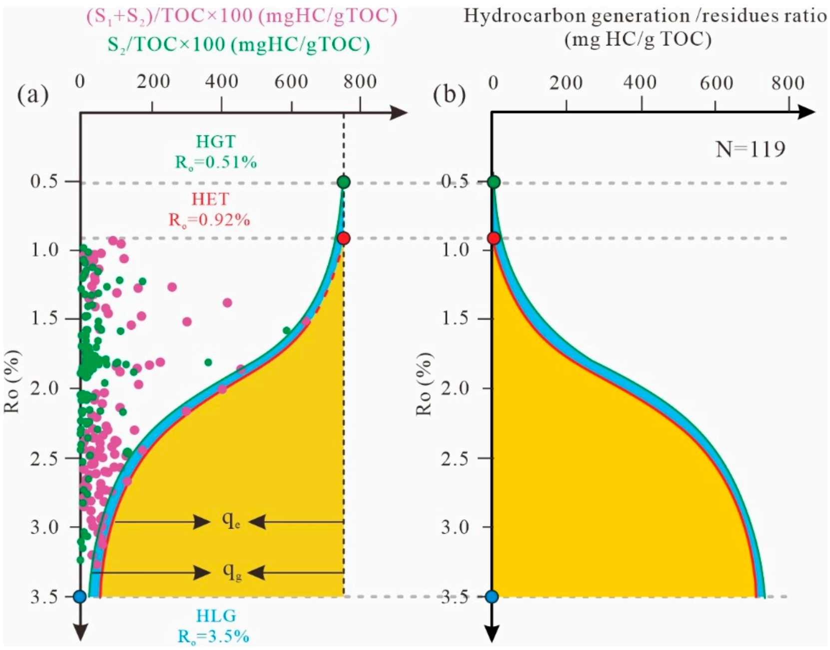

Figure 10. Model for quantifying hydrocarbon generation and residues of Dengying Fm microbial dolomite.

The q_g and q_r of source rocks exhibit a rapid increase during the initial phase of surpassing the HGT and HET, respectively, followed by a stabilization in the later stages (Figure 10b). Prior to crossing the HET, most of the petroleum is retained within the source rocks, with only a small fraction of hydrocarbons being expelled. However, with increased burial depth, a significant portion of the hydrocarbons previously held in the source rocks are progressively liberated.

4.2.2. Hydrocarbon Generation Intensities and Amount of Source Rocks

The conceptual model provides insights into the hydrocarbon generation and residue features under varying thermal conditions [53]. Integrating the burial history and thermal evolution trajectory of the Sichuan Basin [1] allows us to comprehend the hydrocarbon generation characteristics across different geological eras. The Ediacaran Dengying Fm microbial dolomite in the Sichuan Basin experienced two periods of structural uplift in the Ordovician and the Jurassic, respectively, and there are four main eras of hydrocarbon generation. Using geological data on the thickness of source rocks and the geological data of TOC, we can compute the hydrocarbon generation intensity and hydrocarbon generation quantity in different geological periods through Equations (1), (4), and (6).

During the early Cambrian, the microbial dolomite entered the hydrocarbon generation threshold, and the corresponding thermal evolution R_o was 0.51%. The Caledonian movement during the Silurian period caused the basin to be uplifted and eroded. The duration was as long as 140 Ma, after which time the microbial dolomite hydrocarbon generation ceased. In Figure 11a, the hydrocarbon generation intensity for microbial dolomites at the end of the Silurian is depicted. The central areas of the Sichuan Basin exhibited a prominent hydrocarbon generation center, surpassing 1.8×10^7 t/km^2, gradually diminishing towards the basin's periphery. Moving into the Permian period, during the rapid subsidence of the Ediacaran, occurring at a speed of 60 m/Ma, microbial dolomites commenced hydrocarbon regeneration. By the Triassic, two hydrocarbon-generating centers emerged in the central and northern regions of the Sichuan Basin, with generation intensities of 1.7×10^7 t/km^2 and 2.1×10^7 t/km^2, respectively (Figure 11b).

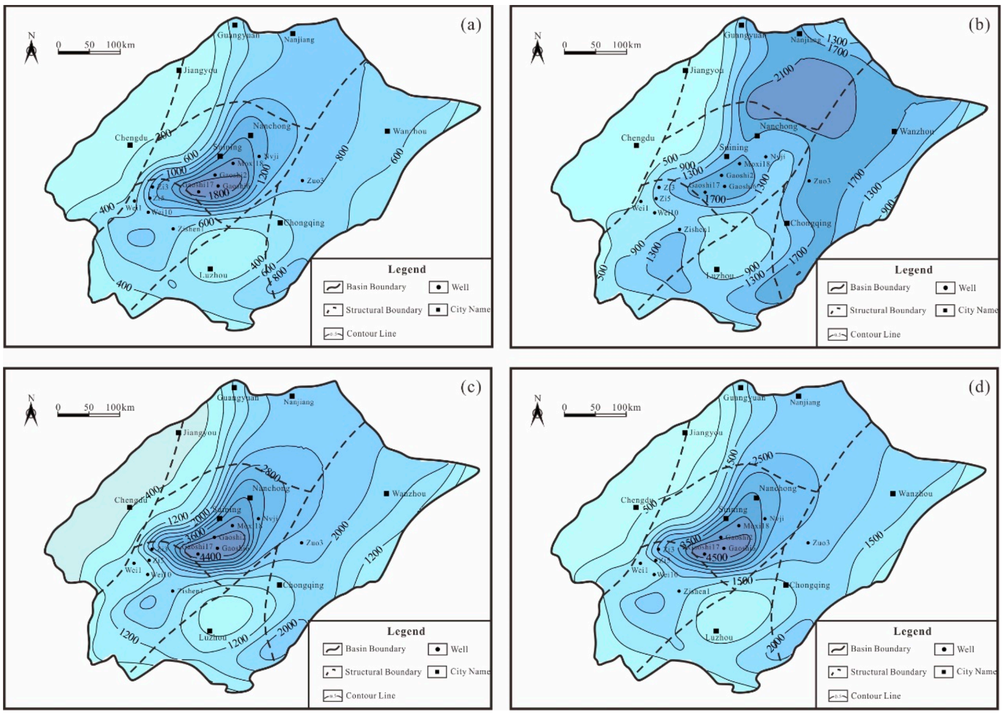

Figure 11. Hydrocarbon generation intensity of the microbial dolomite of the Dengying Fm in the Sichuan Basin. The panels delineate hydrocarbon generation intensities (10^4 t/km^2) for various geological periods: (**a**) Silurian, (**b**) Triassic, (**c**) Jurassic, and (**d**) Present day.

As illustrated in Figure 11c, towards the end of the Jurassic, only one hydrocarbon generation center, referring to the area with the maximum hydrocarbon generation intensity, was situated in the central areas of the Sichuan Basin, boasting a hydrocarbon generation intensity of 4.4×10^7 t/km^2. The Late Cretaceous Himalayan movement induced a substantial uplift in the basin, leading to a cessation of hydrocarbon generation. Consequently, the hydrocarbon generation intensities remained consistent from the end of the Cretaceous to the present day. The center, primarily located in the central areas of the Sichuan Basin, maintained an intensity of 4.5×10^7 t/km^2 (Figure 11d).

Using Equation (6), we computed the cumulative hydrocarbon generation amounts of microbial dolomite in history, as presented in Table 3. The hydrocarbon generation amounts from Ediacaran Dengying Fm microbial dolomite source rocks during various time periods, along with the cumulative amounts, are illustrated in Figure 12. The findings demonstrate three significant stages of hydrocarbon generation in the Ediacaran microbial dolomite source rock in the Sichuan Basin: Silurian, Triassic, and Jurassic. The hydrocarbon generation amounts for these separate stages are 1.05×10^{12} t, 9.5×10^{11} t, and 6.49×10^{11} t, respectively.

Table 3. Hydrocarbon generation amount of the microbial dolomite of the Dengying Formation in different geological periods.

Hydrocarbon Generation	Silurian	Triassic	Jurassic	Present Day
Cumulative amount (10^8 t)	10,535.3	20,079.5	26,576.3	27,089.9

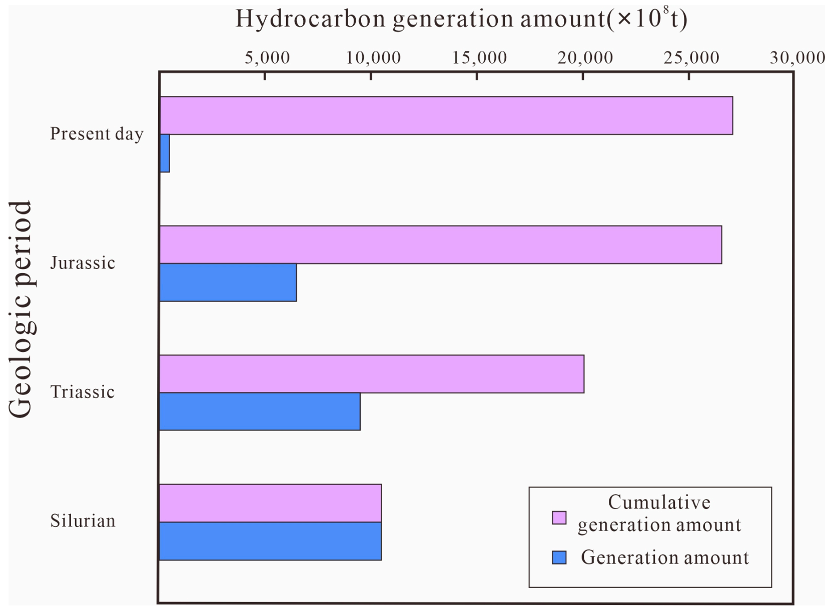

Figure 12. Hydrocarbon generation amounts in the microbial dolomite for different geological periods.

4.2.3. Hydrocarbon Residue Intensities and Amount of Source Rocks

By using the TOC and thickness data, the hydrocarbon residue ratio, the hydrocarbon residue intensity and amount can be calculated according to Equations (2) and (5). The hydrocarbon residue intensity of the Ediacaran microbial dolomites is shown in Figure 13. One hydrocarbon residue center was present, in the central areas of the Sichuan Basin, with hydrocarbon residue intensities of 3.2×10^7 t/km^2. The hydrocarbon residue amounts of the Ediacaran Dengying Fm microbial dolomite are calculated based on Equation (7), which is 1.66×10^{12} t.

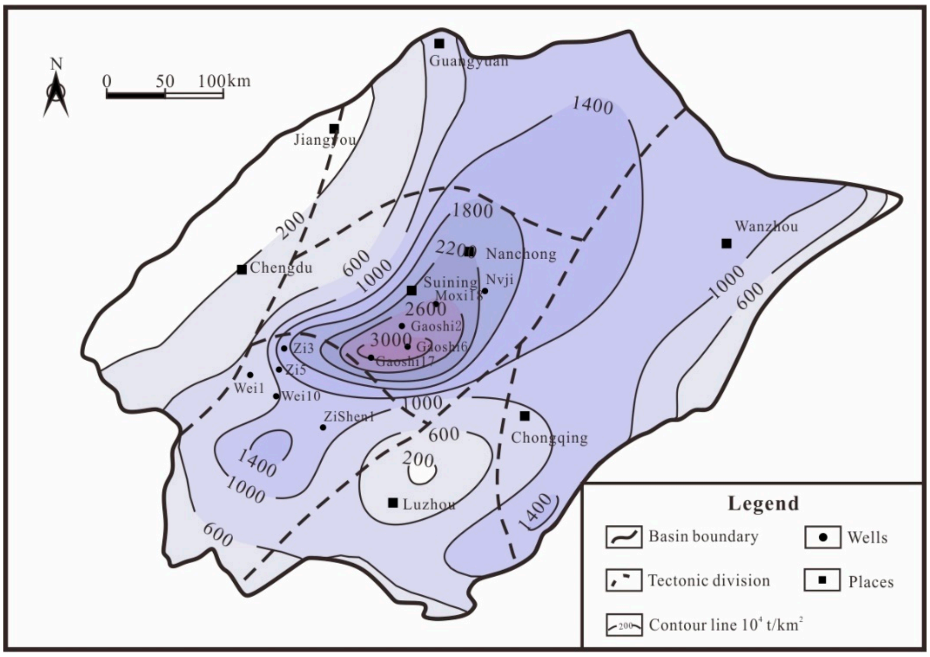

Figure 13. Hydrocarbon residue intensity of the microbial dolomite of the Dengying Fm in the Sichuan Basin (10^4 t/km^2).

5. Discussion

5.1. Ediacaran Microbial Dolomite Resource Potential in the Sichuan Basin

The Dengying Fm in the Sichuan Basin boasts favorable petroleum geological conditions, making it conducive to natural gas formation [13,73,74]. Based on the model discussed in Section 4.2, the Ediacaran microbial dolomite in the Sichuan Basin has the potential to generate approximately 2.7×10^{12} t of hydrocarbons (Table 1). Taking into account an aggregation coefficient of 1% for hydrocarbon accumulation in the deep marine strata [1], we assessed the resources within the Ediacaran Dengying Fm microbial dolomite in the Sichuan Basin. The estimated amount ranges from 270×10^8 t (equivalent to 33.8×10^{12} m^3), underscoring a significant resource potential. Shi et al. [4] believed that the Ediacaran microbial dolomite in the Sichuan basin was a set of potential hydrocarbon sources. The results of our study align with this perspective, portraying the Ediacaran Dengying Fm microbial dolomite in the Sichuan Basin as robust source rocks that have generated substantial hydrocarbons, thus holding promising exploration potential.

5.2. Prospects of Ediacaran Gas Exploration in the Sichuan Basin

Source rocks exert significant control over the distribution range of hydrocarbon accumulation [34,75,76]. In conventional hydrocarbon accumulation scenarios, hydrocarbons are expelled from source rocks and migrate to reservoirs, and the prospects are influenced by the hydrocarbon generation intensity of these source rocks [54]. Favorable zones are strategically located at an optimal distance from the source rocks exhibiting the highest hydrocarbon generation intensity [54]. These geological conditions are conducive to the formation of high-quality reservoirs [12].

However, for the source-reservoir assemblage type of resource [76,77], the prospects are dictated by the hydrocarbon residue intensity within the source rocks [76]. Favorable zones are identified within the source rocks with the highest hydrocarbon residue intensity [76]. In this context, the central district of the Sichuan Basin has been identified as a potential area within the Ediacaran Dengying Formation, demonstrating favorable conditions for future exploration (Figure 13).

5.3. Insights for Gas Exploration in Areas with High-Maturity Source Rocks

In regions where source rocks have undergone significant thermal maturation, the TOC in the rocks decreases due to hydrocarbon expulsion. This results in a 'high in ancient times and low today' TOC scenario. Essentially, when these rocks were initially formed, their TOC content was very high; however, the measured TOC today is considerably lower, making it easy to misidentify them as ineffective source rocks. This is in stark contrast to the 'low in ancient times and low in present' TOC characteristics, which pertain to rocks that had a low initial TOC due to the absence of organic matter during their formation, rendering them ineffective source rocks. Therefore, evaluating highly mature source rocks solely based on TOC indices can lead to significant errors. It is essential to comprehensively assess the residual hydrocarbon generation and expulsion throughout the historical process. Effective evaluation should consider whether the historical hydrocarbon expulsion exceeds zero and meets industrial accumulation standards. Rocks that meet these criteria are considered effective hydrocarbon source rocks. Moreover, if the residual hydrocarbon content surpasses zero and aligns with industrial accumulation standards, these rocks become viable targets for shale oil and gas exploration, warranting special attention.

In addition, there is a worldwide lack of low-maturity source rocks in Precambrian formations. It is a crucial challenge to locate ancient, low-maturity source rock samples, conduct hydrocarbon generation thermal simulation experiments to ascertain their original hydrocarbon generation potential and validate the abundance of organic matter and resource potential in ancient formations. Additionally, this article proposes the hydrocarbon generation potential of microbial dolomite from the perspective of hydrocarbon generation and expulsion. Traditionally, this type of rock has been regarded as a reservoir, so our proposal represents a relatively recent viewpoint. In future research, efforts will be intensified in the investigation of paleoenvironments, organic and inorganic isotopes, and residual bitumen to further substantiate its classification as an effective source rock.

6. Conclusions

The Ediacaran microbial dolomite within the Sichuan Basin's Dengying Formation stands out as a favorable source rock, displaying significant hydrocarbon generation and residue potential. Formed within a saline marine reducing environment, this dolomite is extensively spread across the Sichuan Basin, averaging a thickness of 251 m. Characterized by an average TOC of 0.82%, the kerogen is primarily identified as type I, with a minor presence of type II. Its thermal evolution has progressed to the post-maturity stage.

Significant hydrocarbon generation and residues have transpired within the geological history of the Ediacaran Dengying microbial dolomite in the Sichuan Basin. The maximum intensities for hydrocarbon generation and residues reached 4500×10^4 t/km^2 and 3200×10^4 t/km^2, respectively. Furthermore, the total amounts of generated and residual hydrocarbons amounted to 2.7×10^{12} t and 1.67×10^{12} t, respectively. The Ediacaran Dengying Formation holds substantial exploration potential, particularly within the central district of the Sichuan Basin, identified as a promising area for future exploration.

Author Contributions: Conceptualization, W.W. and X.P.; methodology, W.W. and Y.W.; software, M.C., C.L. and Y.C.; writing—review and editing, W.W. and Z.C.; funding acquisition, W.W. All authors have read and agreed to the published version of the manuscript.

Funding: This research was funded by [Open Fund Project of the State Key Laboratory of Lithospheric Evolution] grant number [SKL-K202103].

Data Availability Statement: Data is contained within the article.

Conflicts of Interest: The authors declare that they have no known competing financial interests.

References

1. Zou, C.N.; Wei, G.Q.; Xu, C.C.; Du, J.H.; Xie, Z.Y.; Wang, Z.C.; Hou, L.H.; Yang, C.; Li, J.; Yang, W. Geochemistry of the Ediacaran–cambrian gas system in the Sichuan basin, China. *Org. Geochem.* **2014**, *74*, 13–21. [CrossRef]

2. Hoshino, Y.; Poshibaeva, A.; Meredith, W.; Snape, C.; Poshibaev, V.; Versteegh, G.; Kuznetsov, N.; Leider, A.; van Maldegem, L.; Neumann, M.; et al. Cryogenian evolution of stigmasteroid biosynthesis. *Sci. Adv.* **2017**, *3*, e1700887. [CrossRef]
3. Canfield, D.E.; Zhang, S.C.; Frank, A.B.; Wang, X.M.; Wang, H.J.; Su, J.; Ye, Y.T.; Frei, R. Highly fractionated chromium isotopes in Mesoproterozoic-aged shales and atmospheric oxygen. *Nat. Commun.* **2018**, *9*, 2871. [CrossRef]
4. Shi, C.H.; Cao, J.; Tan, X.C.; Luo, B.; Zeng, W.; Hong, H.T.; Huang, X.; Wang, Y. Hydrocarbon generation capability of Ediacaran–Lower Cambrian shale, mudstone, and carbonate rocks in the Sichuan Basin, southwestern China: Implications for contributions to the giant Ediacaran Dengying natural gas accumulation. *AAPG Bull.* **2018**, *102*, 817–853. [CrossRef]
5. Zhang, F.; Xiao, S.; Kendall, B.; Romaniello, S.J.; Cui, H.; Meyer, M.; Gilleaudeau, G.J.; Kaufman, A.J.; Anbar, A.D. Extensive marine anoxia during the terminal Ediacaran Period. *Sci. Adv.* **2018**, *4*, eaan8983. [CrossRef]
6. Galili, N.; Shemesh, A.; Yam, R.; Brailovsky, I.; Sela-Adler, M.; Schuster, E.M.; Collom, C.; Bekker, A.; Planavsky, N.; Macdonald, F.A.; et al. The geologic history of seawater oxygen isotopes from marine iron oxides. *Science* **2019**, *365*, 469–473. [CrossRef]
7. Grosjean, E.; Love, G.D.; Stalvies, C.; Fike, D.A.; Summons, R.E. Origin of petroleum in the Neoproterozoic–Cambrian South Oman salt basin. *Org. Geochem.* **2009**, *40*, 87–110. [CrossRef]
8. Craig, J.; Biffi, U.; Galimberti, R.F.; Ghori, K.A.R.; Gorter, J.D.; Hakhoo, N.; Heron, D.P.L.; Thurow, J.; Vecoli, M. The palaeobiology and geochemistry of Precambrian hydrocarbon source rocks. *Mar. Pet. Geol.* **2013**, *40*, 1–47. [CrossRef]
9. Kelly, A.E.; Love, G.D.; Zumberge, J.E.; Summons, R.E. Hydrocarbon biomarkers of Neoproterozoic to Lower Cambrian oils from eastern Siberia. *Org. Geochem.* **2011**, *42*, 640–654. [CrossRef]
10. Dutta, S.; Bhattacharya, S.; Raju, S.V. Biomarker signatures from Neoproterozoic–early Cambrian oil, western India. *Org. Geochem.* **2013**, *56*, 68–80. [CrossRef]
11. Katz, B.J.; Everett, M.A. An overview of pre-Devonian petroleum systems–Unique characteristics and elevated risks. *Mar. Pet. Geol.* **2016**, *73*, 492–516. [CrossRef]
12. Wang, W.Y.; Pang, X.Q.; Chen, Z.X.; Chen, D.X.; Zhen, T.Y.; Luo, B.; Li, J.; Yu, R. Quantitative Prediction of Oil and Gas Prospects of the Ediacaran-Lower Paleozoic in the Sichuan Basin in Central China. *Energy* **2019**, *174*, 861–872. [CrossRef]
13. Zou, C.N.; Du, J.H.; Xu, C.C.; Wang, Z.C.; Zhang, B.M.; Wei, G.Q.; Wang, T.S.; Yao, G.S.; Deng, S.H.; Liu, J.J.; et al. Formation, distribution, resource potential, and discovery of Ediacaran–Cambrian giant gas field, Sichuan Basin, SW China. *Pet. Explor. Dev.* **2014**, *41*, 306–325. [CrossRef]
14. Luo, B.; Luo, W.J.; Wang, W.Z.; Wang, Z.H.; Shan, S.J. Formation mechanism of the Ediacaran natural gas reservoir in the Leshan-Longnvsi Paleo-uplift, Sichuan Basin. *Nat. Gas Geosci.* **2015**, *26*, 444–455. (In Chinese with English Abstract)
15. Wright, M.C.; Court, R.W.; Kafantaris, F.C.A.; Spathopoulos, F. A new rapid method for shale oil and shale gas assessment. *Fuel* **2015**, *153*, 231–239. [CrossRef]
16. Li, W.H.; Lu, S.F.; Xue, H.T.; Zhang, P. Oil content in argillaceous dolomite from the Jianghan Basin, China: Application of new grading evaluation criteria to study shale oil potential. *Fuel* **2015**, *143*, 424–429. [CrossRef]
17. Sun, C.; Nie, H.; Dang, W.; Chen, Q.; Zhang, G.; Li, W.; Lu, Z. Shale gas exploration and development in China: Current status, geological challenges, and future directions. *Energy Fuels* **2021**, *35*, 6359–6379. [CrossRef]
18. Zou, S.; Yao, P.; Wang, D.; Zhang, X.; Ge, D.; Chen, Y.; Zhang, J.; Chen, H.; Kong, F.; Liu, Z.; et al. Physical Properties of Hydrocarbon Source Reservoir in the Lucaogou Formation in Junggar Basin (China) and Its Influence on Adsorption Ability and Surface Free Energy. *Processes* **2023**, *11*, 2832. [CrossRef]
19. Prischepa, O.; Nefedov, Y.; Nikiforova, V.; Ruiming, X. Raw material base of Russia's unconventional oil and gas reserves (hydrocarbons shale strata). *Front. Earth Sci.* **2022**, *10*, 958315. [CrossRef]
20. Dai, J.X. Pool forming period and gas sources of Weiyuan Gasfield. *Pet. Geol. Exp.* **2003**, *25*, 473–479. (In Chinese with English Abstract)
21. Liu, R.B.; Tian, J.C.; Wei, Z.H.; Zhang, M.W.; Zhong, S.Q.; Zhang, G.H.; Wang, B. Comprehensive research of effective hydrocarbon source rock of lower strata from Ediacaran to Silurian System in southeast area of Sichuan Province. *Nat. Gas Geosci.* **2006**, *17*, 824–828.
22. Xu, G.S.; Yuan, H.F.; Ma, Y.S.; Liu, S.G.; Cai, X.Y.; Wang, G.Z.; Pan, C.L. The source of Ediacaran and Lower-Palaeozoic bitumen and hydrocarbon evolution in the middle and southeast of the Sichuan basin. *Acta Geol. Sin.* **2007**, *81*, 1143–1152.
23. Liu, D.; Xie, Z.Y.; Li, J.; Chen, J.A. The Inorganic Microelement Characteristics and Hydrocarbon Potential Prediction of Microbial dolomite in Dengying Formation from Sichuan Basin. *Sci. Technol. Eng.* **2013**, *13*, 2791–2798.
24. Wang, E.; Li, Y.; Guo, T.; Xiong, L.; Dong, X.; Wang, T.; Shi, K. Geological Features, Paleosedimentary Environment, and Organic Matter Accumulation Mechanisms of the Lacustrine Shale Oil System: A Case Study of the Jurassic Dongyuemiao Member in the Sichuan Basin. *Processes* **2023**, *11*, 2638. [CrossRef]
25. Tian, X.W.; Hu, G.Y.; Li, W.; Li, X.Q.; Su, G.P.; Xu, Y.R.; Cai, D.; Wei, H.P. Geochemical Characteristics and Significance of Simian Reservoir bitumen in Leshan-Longvsi Paleo-uplift Area, Sichuan Basin. *Nat. Gas Geosci.* **2013**, *24*, 982–990.
26. Liu, D.; Li, J.; Xie, Z.Y.; Guo, J.Y.; Hao, A.S. Origin and significance of Ediacaran original and coexist bitumen of central Sichuan Basin. *Pet. Geol. Exp.* **2014**, *36*, 218–223.
27. Peters, K.E.; Clark, M.E.; Das Gupta, U.; McCaffrey, M.A.; Lee, C.Y. Recognition of an Infracambrian source rock based on biomarkers in the Baghewala-1 oil, India. *AAPG Bull.* **1995**, *79*, 1481–1493.
28. Słowakiewicz, M.; Mikołajewski, Z. Upper Permian Main Dolomite microbial carbonates as potential source rocks for hydrocarbons (W. Poland). *Mar. Pet. Geol.* **2011**, *28*, 1572–1591. [CrossRef]

29. Pan, Y.; Huang, Z.; Li, T.; Xu, X.F.; Guo, X.B.; Wang, R.; Zheng, H.R.; Zhang, W. Study on the origin and hydrocarbon generation potential of lacustrine organic-rich dolomite affected by volcanism: A case study of Lucaogou Formation in the Malang Sag, Santanghu Basin, Western China. *Mar. Pet. Geol.* **2022**, *141*, 105699. [CrossRef]
30. Liu, S.G.; Ma, Y.S.; Cai, X.Y.; Xu, G.S.; Wang, G.Z.; Yong, Z.Q.; Sun, W.; Yuan, H.F.; Pan, C.L. Characteristic and accumulation process of the natural gas from Ediacaran to Lower Paleozoic in Sichuan Basin. *J. Chengdu Univ. Technol. Sci. Technol. Ed.* **2009**, *36*, 345–354.
31. Wei, G.Q.; Jiao, G.H.; Yang, W.; Xie, Z.Y.; Li, D.J.; Xie, W.R.; Liu, M.C.; Zeng, Y. Hydrocarbon pooling conditions and exploration potential of Ediacaran-Lower Paleozoic gas reservoirs in the Sichuan Basin. *Nat. Gas Ind.* **2010**, *30*, 5–9.
32. Lafargue, E.; Espitalié, J.; Jacobsen, T.; Eggen, S. Experimental simulation of hydrocarbon expulsion. *Org. Geochem.* **1990**, *16*, 121–131. [CrossRef]
33. Peters, K.E.; Burnham, A.K.; Walters, C.C. Petroleum generation kinetics: Single versus multiple heating-ramp open-system pyrolysis: Reply. *AAPG Bull.* **2016**, *100*, 690–694. [CrossRef]
34. Peters, K.E.; Burnham, A.K.; Walters, C.C. Petroleum generation kinetics: Single versus multiple heating-ramp open-system pyrolysis. *AAPG Bull.* **2015**, *99*, 591–616. [CrossRef]
35. Waples, D.W. Petroleum generation kinetics: Single versus multiple heating-ramp open-system pyrolysis: Discussion. *AAPG Bull.* **2016**, *100*, 683–689. [CrossRef]
36. Lehne, E.; Dieckmann, V. Bulk kinetic parameters and structural moieties of asphaltenes and kerogens from a sulphur-rich source rock sequence and related petroleums. *Org. Geochem.* **2007**, *38*, 1657–1679. [CrossRef]
37. Rao, S.; Hu, S.B.; Wang, J.Y. Hydrocarbon generation kinetic parameters of organic matter: Review and outlook. *Prog. Geophys.* **2010**, *25*, 1424–1432. (In Chinese with English Abstract)
38. Makeen, Y.M.; Abdullah, W.H.; Hakimi, M.H.; Mustapha, K.A. Source rock characteristics of the Lower Cretaceous Abu Gabra Formation in the Muglad Basin, Sudan, and its relevance to oil generation studies. *Mar. Pet. Geol.* **2015**, *59*, 505–516. [CrossRef]
39. Liu, B.; Mahlstedt, N.; Horsfield, B.; Tian, S.S.; Huo, Q.L.; Wen, Z.G.; Pan, Z.J. Phase behavior and GOR evolution using a natural maturity series of lacustrine oil-prone shale: Implications from compositional modelling. *Org. Geochem.* **2023**, *185*, 104675. [CrossRef]
40. Yan, X.P.; Kang, Y.L.; You, L.J.; Xu, C.Y.; Lin, C.; Zhang, J.Y. Drill-in fluid loss mechanisms in brittle gas shale: A case study in the Longmaxi Formation, Sichuan Basin, China. *J. Pet. Sci. Eng.* **2019**, *174*, 394–405. [CrossRef]
41. Ma, Y.S.; Guo, X.S.; Guo, T.L.; Huang, R.; Cai, X.Y.; Li, G.X. The Puguang gas field: New giant discovery in the mature Sichuan Basin, southwest China. *AAPG Bull.* **2007**, *91*, 627–643. [CrossRef]
42. Hao, F.; Guo, T.L.; Zhu, Y.M.; Cai, X.Y.; Zou, H.Y.; Li, P.P. Evidence for multiple stages of oil cracking and thermochemical sulfate reduction in the Puguang gas field, Sichuan Basin, China. *AAPG Bull.* **2008**, *92*, 611–637. [CrossRef]
43. Wang, L.Q.; Fan, C.H.; Fan, Z.H.; Jiang, B. Presumption of the tectonic evolution and regional sedimentation of the Sichuan Basin based on seismic exploration technology. *Nat. Gas Ind.* **2016**, *7*, 18–26.
44. Mei, M.X.; Zhou, P.; Zhang, H.; Chen, Y.H.; Nie, R.Z. Sequence stratigraphic framework and its palaeogeographical background for the Ediacaran of Upper Yangtze Region. *J. Paleogeogr.* **2006**, *8*, 219–231.
45. Du, J.H.; Zou, X.N.; Xu, C.C.; He, H.Q.; Shen, P.; Yang, Y.M.; Li, Y.L.; Wei, G.Q.; Wang, Z.C.; Yang, Y. Theoretical and technical innovations in strategic discovery of a giant gas field in Cambrian Longwangmiao Formation of central Sichuan paleo-uplift, Sichuan Basin. *Pet. Explor. Dev.* **2014**, *41*, 294–305. [CrossRef]
46. Wang, Y.W. Hydrocarbon Expulsion Characteristics of Sinian and Lower Paleozoic Source Rocks and Their Controlling Effects on Hydrocarbon Accumulations. Master's Thesis, China University of Petroleum, Beijing, China, 2016.
47. Wang, W.Y.; Pang, X.Q.; Wang, Y.P.; Chen, Z.X.; Li, C.R.; Ma, X.H. Hydrocarbon expulsion model and resource potential evaluation of high-maturity marine source rocks in deep basins: Example from the Ediacaran microbial dolomite in the Sichuan Basin, China. *Pet. Sci.* **2022**, *19*, 2618–2630. [CrossRef]
48. Stüeken, E.E.; Zaloumis, J.; Meixnerová, J.; Buick, R. Differential metamorphic effects on nitrogen isotopes in kerogen extracts and bulk rocks. *Geochim. Cosmochim. Acta* **2017**, *217*, 80–94. [CrossRef]
49. Chen, J.; Chen, J.; Yao, L.; Luo, Q.; Shi, S.; Chen, J.; Zhu, L.; Chen, Z. Influencing factors and significance of organic and inorganic nitrogen isotopic compositions in lacustrine sedimentary rocks. *Geosci. Front.* **2023**, *14*, 101501. [CrossRef]
50. Durand, B. *Kerogen: Insoluble Organic Matter from Sedimentary Rocks*; Editions Technip.: Paris, France, 1980.
51. Vandenbroucke, M.; Largeau, C. Kerogen origin, evolution and structure. *Org. Geochem.* **2007**, *38*, 719–833. [CrossRef]
52. Li, C.; Pang, X.; Ma, X.; Wang, E.; Hu, T.; Wu, Z. Hydrocarbon generation and expulsion characteristics of the Lower Cambrian Qiongzhusi shale in the Sichuan Basin, Central China: Implications for conventional and unconventional natural gas resource potential. *J. Pet. Sci. Eng.* **2021**, *204*, 108610. [CrossRef]
53. Pang, X.Q.; Li, M.W.; Li, S.M.; Jin, Z.J. Geochemistry of petroleum systems in the Niuzhuang South Slope of Bohai Bay Basin: Part 3. Estimating hydrocarbon expulsion from the Shahejie formation. *Org. Geochem.* **2005**, *36*, 497–510. [CrossRef]
54. Jiang, F.J.; Pang, X.Q.; Bai, J.; Zhou, X.Y.; Li, J.P.; Guo, Y.H. Comprehensive assessment of source rocks in the Bohai Sea area, Eastern China. *AAPG Bull.* **2016**, *100*, 969–1002.
55. Xia, L.W.; Cao, J.; Wang, M.; Mi, J.L.; Wang, T.T. A review of carbonates as hydrocarbon source rocks: Basic geochemistry and oil–gas generation. *Pet. Sci.* **2019**, *16*, 713–728. [CrossRef]

56. Li, Y.H.; Yang, W.; Wang, Q.Y.; Song, Y.; Jiang, Z.X.; Guo, L.S.; Zhang, Y.; Wang, J.B. Influence of the actively migrated diagenetic elements on the hydrocarbon generation potential in tuffaceous shale. *Fuel* **2019**, *256*, 115795. [CrossRef]
57. Espitalié, J.; Marquis, F.; Sage, L.; Barsony, I. Géochimie organique du bassin de paris. *Oil Gas Sci. Technol.* **1987**, *42*, 271–302. [CrossRef]
58. Wang, Z.; Zhao, W.; Zhang, L. *Tectonic Sequence and Natural Gas Exploration of Sichuan Basin, Beijing*; Geological Publishing House: Beijing, China, 2002; pp. 13–18.
59. Wang, X.; Huang, J.; Hou, F. Characteristics of deposition and sequence stratigraphy of reservoir interval in S'mian Dengying Formation in Zyang and its neighbouring area. *J. Southwest. Pet. Inst.* **1996**, *18*, 1–9.
60. Breger, I.A. *Organic Geochemistry*; Pergamon Press: Oxford, UK, 1963; pp. 66–100.
61. Shanmugam, G. Significance of coniferous rain forests and related organic matter in generating commercial quantities of oil, Gippsland Basin, Australia. *AAPG Bull.* **1985**, *69*, 1241–1254. [CrossRef]
62. Sahoo, A.K.; Basu, S.; Vishal, V.; Srivastava, M. Hierarchical clustering of Pristane and Phytane data to identify the sweet spots in the shale reservoirs. *Energy Clim. Chang.* **2020**, *1*, 100011. [CrossRef]
63. Obermajer, M.; Fowler, M.G.; Snowdon, L.R. Depositional environment and oil generation in Ordovician source rocks from southwestern Ontario, Canada: Organic geochemical and petrological approach. *AAPG Bull.* **1999**, *83*, 1426–1453.
64. Peters, K.E.; Walters, C.C.; Moldowan, J.M. *Biomarkers and Isotopes in the Petroleum Exploration and Earth History: The Biomarker Guide*, 2nd ed.; Cambridge University Press: Cambridge, UK, 2005; p. 681.
65. Powell, T.G.; Mckirdy, D.M. Relationship between ratio of pristane to phytane, crude oil composition and geological environment in Australia. *Nature* **1973**, *243*, 37–39. [CrossRef]
66. Chen, G.; Gang, W.Z.; Wang, N.; Zhao, L.Y. Geochemical characterization of the Xiagou Formation carbonate-bearing mudstone in southwestern Jiuquan Basin, China: Implications for paleoenvironment reconstruction and the origin of organic matter. *Aust. J. Earth Sci.* **2018**, *65*, 121–134. [CrossRef]
67. Peters, K.E.; Moldowan, J.M. *The Biomarker Guide: Interpreting Molecular Fossils in Petroleum and Ancient Sediments*; Prentice-Hall: Englewood Cliffs, NJ, USA, 1993.
68. Huang, W.Y.; Meinschei, W.G. Sterols as ecological indicators: *Geochim. Cosmochim. Acta* **1979**, *43*, 739–745. [CrossRef]
69. Volkman, J.K.; Barrett, S.M.; Dunstan, G.A.; Jeffrey, S.W. Sterol biomarkers for microalgae from the green algal class Prasinophyceae: *Org. Geochem.* **1994**, *21*, 1211–1218. [CrossRef]
70. Peters, K.E.; Cassa, M.R. Applied Source Rock Geochemistry. In *The Petroleum System—From Source to Trap*; Magoon, L.B., Dow, W.G., Eds.; American Association of Petroleum Geologists: Tulsa, OK, USA, 1994; pp. 93–120.
71. Dai, H.M.; Huang, D.; Liu, X.N.; Yang, Y.; He, X.M.; Peng, H.R.; Tong, J.R. Characteristics and evaluation of marine source rock in southwestern Sichuan. *Nat. Gas Geosci.* **2008**, *19*, 503–508.
72. *SY/T5735–1995*; Geochemistry Evaluation Method for Land Facies Hydrocarbon Source Rock. China National Petroleum Corporation: Beijing, China, 1995.
73. Wei, G.Q.; Yang, W.; Liu, M.C.; Xie, W.R.; Jin, H.; Wu, S.J.; Su, N.; Shen, Y.H.; Hao, C.P. Distribution rules, main controlling factors and exploration directions of giant gas fields in the Sichuan Basin. *Nat. Gas Ind.* **2019**, *6*, 1–12. (In Chinese with English Abstract) [CrossRef]
74. Ma, X.H.; Yang, Y.; Wen, L.; Luo, B. Distribution and exploration direction of medium-and large-sized marine carbonate gas fields in Sichuan Basin, SW China. *Pet. Explor. Dev.* **2019**, *46*, 3–17. [CrossRef]
75. Tissot, B.P.; Welte, D.H. *Petroleum Formation and Occurrence: A New Approach to Oil and Gas Exploration*; Springer: Berlin, Germany, 1978.
76. Zou, C.N.; Yang, Z.; Tao, S.Z.; Li, W.; Wu, S.T.; Hou, L.H.; Zhu, R.; Yuan, X.; Wang, L.; Gao, X.; et al. Nano-hydrocarbon and the accumulation in coexisting source and reservoir. *Pet. Explor. Dev.* **2012**, *39*, 15–32. [CrossRef]
77. Liu, Y.Z.; Zeng, J.H.; Qiao, J.C.; Yang, G.; Liu, S.; Cao, W. An advanced prediction model of shale oil production profile based on source-reservoir assemblages and artificial neural networks. *Appl. Energy* **2023**, *333*, 120604. [CrossRef]